Different Fast-gate Regulation by External Cl^- and H^+ of the Muscle-type ClC Chloride Channels

Mei-Fang Chen[1] and Tsung-Yu Chen[1,2]

[1]Center for Neuroscience and [2]Department of Neurology, University of California, Davis, CA 95616

abstract The fast gate of the muscle-type ClC channels (ClC-0 and ClC-1) opens in response to the change of membrane potential (V). This gating process is intimately associated with the binding of external Cl^- to the channel pore in a way that the occupancy of Cl^- on the binding site increases the channel's open probability (P_o). External H^+ also enhances the fast-gate opening in these channels, prompting a hypothesis that protonation of the binding site may increase the Cl^- binding affinity, and this is possibly the underlying mechanism for the H^+ modulation. However, Cl^- and H^+, modulate the fast-gate P_o-V curve in different ways. Varying the external Cl^- concentrations ($[Cl^-]_o$) shifts the P_o-V curve in parallel along the voltage axis, whereas reducing external pH mainly increases the minimal P_o of the curve. Furthermore, H^+ modulations at saturating and nonsaturating $[Cl^-]_o$ are similar. Thus, the H^+ effect on the fast gating appears not to be a consequence of an increase in the Cl^- binding affinity. We previously found that a hyperpolarization-favored opening process is important to determine the fast-gate P_o of ClC-0 at very negative voltages. This $[Cl^-]_o$-independent mechanism attracted little attention, but it appears to be the opening process that is modulated by external H^+.

key words: channel gating • ClC-0 • ClC-1 • pH regulation • Cl^- dependence

INTRODUCTION

Ion channels catalyze the transportation of small ions across the cell membrane and, in doing so, maintain normal cellular functions. To achieve functional flexibility, these membrane proteins are regulated by a variety of factors, such as transmembrane voltages, mechanical stretches, extracellular or intracellular ligands, and sometimes the small ions in the aqueous solution (Hille, 1992). In vertebrate skeletal muscles, for instance, external Cl^- and H^+ significantly influence the resting membrane conductance and, thus, control the firing pattern of action potentials (Hodgkin and Horowicz, 1959, 1960). Electrophysiological recordings and flux assays have shown that the muscle membrane is more permeable to Cl^- than to K^+ (Hodgkin and Horowicz, 1959; Hutter and Padsha, 1959; Hutter and Noble, 1960), and if the Cl^- conductance is removed, the membrane current shows little change when the pH is altered (Hutter and Warner, 1967, 1972). These early studies indicated that the chloride conductance on the muscle membrane is regulated by extracellular Cl^- and H^+.

Molecular cloning work in the last 10 yr has made significant progress toward understanding the identity of various Cl^- channels. The principal Cl^- channel in the muscle membrane, ClC-1 (Steinmeyer et al., 1991), belongs to the ClC channel family. This muscle channel has a homologue ClC-0 in the *Torpedo* electric organ (Jentsch et al., 1990; O'Neill et al., 1991), which is derived developmentally from skeletal muscle (Jentsch et al., 1995). The biochemical structure of these "muscle-type" Cl^- channels is made up of two identical subunits (Middleton et al., 1994; Fahlke et al., 1997), and the amino acid sequences of ClC-0 and ClC-1 show ~56% identity. The similarity between these two channels is also shown in their functional properties. The opening of both types of channels display "double-barrel"–like activity (Miller, 1982; Miller and White, 1984; Bauer et al., 1991; Ludewig et al., 1996; Middleton et al., 1996; Saviane et al., 1999; Lin and Chen, 2000), which is controlled by two voltage-dependent gating mechanisms (for review see Miller and Richard, 1990; Pusch and Jentsch, 1994; Jentsch et al., 1999; Maduke et al., 2000). In the case of the gating process with faster kinetics, the channel opens and closes on the millisecond time scale, and the gating is modulated by extracellular Cl^-. When $[Cl^-]_o$ is reduced, the opening curve of this "fast gate" is shifted toward a more depolarized membrane potential (Pusch et al., 1995; Chen and Miller, 1996; Rychkov et al., 1996; 1998). For this and other observations, it has been proposed that the binding of Cl^- to the pores of these channels is required for the depolarization-induced channel opening.

Consistent with the early findings on the muscle Cl^- conductance, varying the external pH also affects the fast gating of ClC-1. With macroscopic current record-

Address correspondence to Dr. Tsung-Yu Chen, Center for Neuroscience, University of California, 1544 Newton Court, Davis, California 95616. Fax: (530)757-8827; E-mail: tycchen@ucdavis.edu

J. Gen. Physiol. © The Rockefeller University Press • 0022-1295/2001/07/23/10 $5.00
Volume 118 July 2001 23–32
http://www.jgp.org/cgi/content/full/118/1/23

ings, Rychkov et al. (1996, 1997) showed that the ClC-1 current deactivated to a steady-state level upon membrane hyperpolarization, and the deactivating component diminished as there was an increase of the steady-state component when the external pH was reduced. The open probability (P_o)* of the channel at a low pH was therefore increased, but the effect was obvious mainly in the hyperpolarized voltage range. It was suggested that the enhanced fast-gate open probability might be due to protonation of the aforementioned Cl^- binding site, and this increased the Cl^- binding affinity. Dissociation of Cl^- from the binding site, therefore, is no longer voltage-dependent, leading to a shallower P_o-V curve (Rychkov et al., 1996, 1997).

As external Cl^- appears to control the fast gating of ClC-0 and ClC-1 in the same manner, one would expect that H^+ would have a similar modulatory effect on the fast gating of ClC-0. However, previous studies on ClC-0 have not clearly shown an effect of external H^+ on the fast gating. Miller and White (1980) examined the macroscopic conductance of ClC-0 at a fixed voltage of −30 mV, and found that there was no pH effect between pH ~7.4 and ~6.0. Another study at the single-channel level reported that although internal pH profoundly affected the fast gating of ClC-0, no effect was discernible when the pH of the trans chamber (corresponding to the external side) was raised from pH 7.0 to 10.0 (Hanke and Miller, 1983). These reports did not show a clear external H^+ modulation of the ClC-0 fast gating, nor did they support the hypothesis of protonation of the Cl^- binding site. It is our intention here to examine more rigorously whether external H^+ has a modulation on the fast gating of ClC-0 similar to ClC-1. The possibility that external H^+ modulates the affinity of the Cl^- binding site is also examined.

MATERIALS AND METHODS

Expression of ClC-0 and an Inactivation-suppressed Mutant C212S

The present study focuses on the fast gating of ClC-0. We have isolated the fast gating from the inactivation gating by using an inactivation-suppressed mutant C212S. The construction of the cDNA of the wild-type (WT) channel and the site-directed mutagenesis used to create the C212S mutant have been described previously (Chen, 1998; Lin et al., 1999). For RNA synthesis, the plasmids were linearized by restriction enzyme ScaI (New England Biolab). Capped RNAs were synthesized with T3 polymerase using an mMessage mMachine kit (Ambion Inc.). *Xenopus* oocytes were prepared and injected with RNAs as described previously (Chen, 1998).

Macroscopic Current Recording

Whole oocyte currents were recorded at room temperatures (20–23°C) using standard two-electrode voltage clamp techniques. Microelectrodes were pulled by a PP-83 puller (Narashige) and, when filled with 3 M KCl, had resistance of 0.2–1.0 MΩ. The ground electrodes were connected to the recording chamber via 3-M KCl salt bridges. The recorded current was filtered by the built-in filter of the amplifier (model 725C; Warner Instruments) and was digitized at 1 or 2 kHz using a Digidata 1200 data acquisition board and pClamp6 software (Axon Instruments). The standard solution for the recording of whole oocyte current contained the following (in mM): 98 NaCl, 2 $MgSO_4$, and 5 HEPES. The pH of the solution was titrated by adding NaOH or glutamic acid. To make solutions with a lower Cl^- concentration, part of the NaCl was replaced by sodium glutamate. When a higher Cl^- concentration such as 300 mM was needed, NaCl was added to the standard solution to obtain the desired concentration. Because the channel is open at the holding potential, a change of $[Cl^-]_o$ inevitably leads to an alteration of the internal Cl^- concentration ($[Cl^-]_i$). Based on the measured reversal potentials at a steady-state, we estimated that effective $[Cl^-]_i$ were ~60–70, ~36–48, and ~15–20 mM when $[Cl^-]_o$ were 300, 98, and 15 mM, respectively.

To examine the quasi steady-state inactivation curve of the channel (see Fig. 1), a protocol modified from a previously described method (Pusch et al., 1997; Chen, 1998) was used. The membrane potential (V) was held at −30 mV, and a 3.5-s prepulse from 0 to −140 mV in −10-mV steps was followed by a 0.4-s test pulse at +60 mV. The current was measured at the end of the +60-mV test pulse, and was normalized to the maximal current obtained at pH 7.6.

The fast-gating properties of the channel were evaluated with a voltage protocol described before (Chen, 1998; Lin et al., 1999; Lin and Chen, 2000). In brief, multiple short negative voltages were first applied to open the inactivation gate before the experiment. A −120-mV voltage step was applied for 300 ms to ensure the opening of the inactivation gate. The voltage was then clamped at +80 mV for 100 ms, followed by 200-ms test voltages from +120 (or +80) to −160 mV in −20-mV steps. The voltage protocol was completed by a tail voltage step at −100 mV. The recorded current trace was shown only from 80 ms before the start of the test pulse to 200 ms after the end of the test voltage (see Fig. 2 A and Fig. 3). In Fig. 2 A, the tail current traces were enlarged from 20 ms before until 50 ms after the end of the test pulse. For deriving the fast-gate P_o, the tail currents were fitted to a single-exponential function, and their initial values were obtained by extrapolation. These initial tail currents were normalized to the maximal one obtained following the most depolarized test potential (+80 or +120 mV). To estimate the opening and closing rates of the fast gate, the relaxation time constant (τ) was first determined by fitting the current deactivation process to a single-exponential function. The opening rate (α) and closing rate (β), thus, were calculated according to:

$$\alpha = P_o/\tau, \tag{1a}$$

$$\beta = (1 - P_o)/\tau. \tag{1b}$$

However, this method was limited by the degree of the current deactivation. When the membrane potential is more depolarized than −40 mV, or when the external pH is <5, the current deactivation component is so small that the time constant cannot be reliably estimated. The opening and closing rates, thus, cannot be obtained under these conditions.

Single-channel Recordings

The single-channel behavior of the channel was examined at room temperatures (19–23°C) using excised inside-out patch recording

**Abbreviations used in this paper*: P_o, open probability; WT, wild-type.

techniques (Hamill et al., 1981). Detailed procedures were similar to those described previously (Lin et al., 1999; Lin and Chen, 2000). Briefly, the pipet (external) solution contained the following (in mM): 110 NMDG-Cl, 5 $MgCl_2$, 1 $CaCl_2$, and 5 HEPES, pH 5.6–9.6. The bath (internal) solution contained the following (in mM): 110 NaCl, 5 $MgCl_2$, 1 EGTA, and 5 HEPES, pH 7.6. The pH of the internal and external solutions were titrated with NaOH and NMDG, respectively. The current was filtered at 200 Hz (4 pole Bessel) and was digitized by an acquisition board (model DAP 800; Microstar Laboratories, Inc.) at 1 kHz with homemade software (Chen and Miller, 1996; Lin et al., 1999; Lin and Chen, 2000). For the C212S mutant, the dwell-time distribution of the nonconducting events always followed a single-exponential function, indicating that the inactivation was suppressed in this point mutant (Lin et al., 1999). Although the single-channel recording trace shows three equidistant current levels, it is still possible to derive fast-gating parameters assuming the presence of double barrels and independent gating of the two protopores. Accordingly, the P_o of the fast gate is determined from Eq. 2:

$$P_o = f_1/2 + f_2, \tag{2}$$

where f_1 and f_2 represent the probabilities of the intermediate and the fully open levels, respectively. Intuitively, the opening rate (α) and closing rate (β) are as follows:

$$\alpha = 1/(2\tau_0), \tag{3a}$$

$$\beta = 1/(2\tau_2), \tag{3b}$$

where τ_0 and τ_2 are the time constants of the distributions of nonconducting and fully open events, respectively. However, in the very acidic condition (pH = 5.6), τ_0 was difficult to obtain because P_o became so large that the closed events were rare. We exploited the fact that events at the middle level occurred more frequently and also had a longer dwell time than those at the zero current level. The time constant of the dwell-time distribution of the middle level τ_1, therefore, was determined and the opening and closing rates were calculated according to a method described in Chen and Miller (1996):

$$\alpha = P_o/\tau_1, \tag{3c}$$

$$\beta = (1 - P_o)/\tau_1. \tag{3d}$$

Under experimental conditions where both τ_0 and τ_1 can be reliably obtained, α and β were calculated using both these methods (Eqs. 3 a and 3b versus Eqs. 3c and 3d) and agreed within 10% (for the comparison of these two methods also see Chen and Miller, 1996).

Data Analysis

Data analysis of the macroscopic current was conducted using the software programs, pClamp6 (Axon Instruments) and Origin 4.0 (Microcal Software, Inc.). Analysis of the single-channel recording trace was performed using a homemade program (Chen and Miller, 1996; Lin et al., 1999; Lin and Chen, 2000). Because single-channel current amplitudes at voltages close to the reversal potential (0 mV) are small, the single-channel traces were further digitally filtered at 200 Hz, leading to a final filter frequency at ~140 Hz (−3dB). We did not correct the missed events since the change in opening rate by H^+ was much greater than the error that resulted from filtering the recording traces. A previous single-channel recording study using the same digitizing rate and a similar cutoff frequency was shown to have an estimated error for the opening rates of ~5–6% (Chen and Miller, 1996).

Single-channel current amplitudes were determined from all-points amplitude histograms and the time constants of the three current levels were estimated from the dwell-time distribution. All nonconducting events of C212S were included in the analysis because the inactivation of this mutant is suppressed (Lin et al., 1999). All results shown in the figures are presented as mean ± SEM. Curve fitting was performed with an unweighted least-squares method. In fitting the opening rates with Eq. 4 (see Fig. 8, B and C), multiple datasets obtained at different pHs were fitted at the same time, with a shared $\gamma(0)$ in each dataset. See Fig. 8 legend for a detailed description.

RESULTS

Inactivation of C212S Mutant Is Suppressed in Nonphysiological Conditions

In the attempt to isolate the H^+ and Cl^- effects on the fast gating of ClC-0, we face a problem due to the inactivation of the channel. In ClC-0, the inactivation mech-

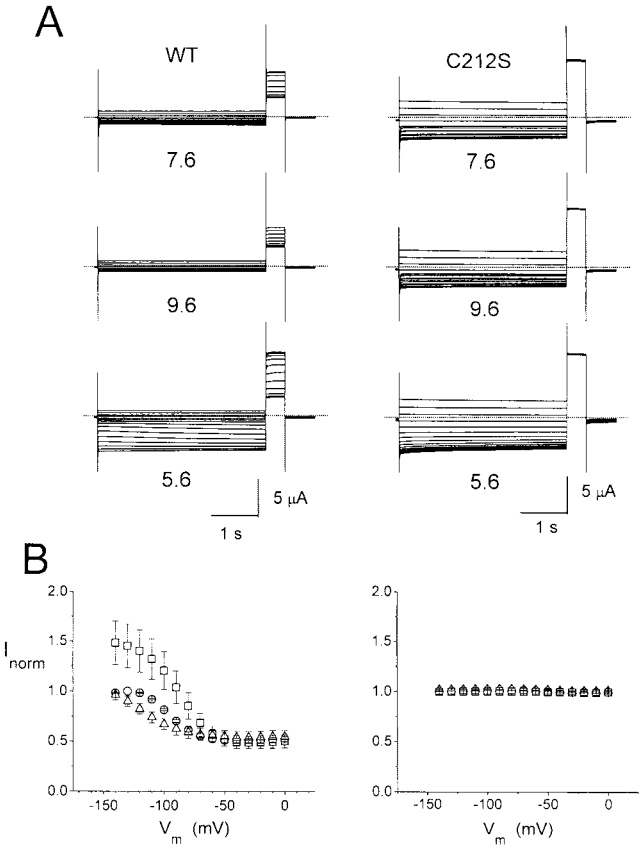

FIGURE 1. Quasi steady-state inactivation curves of the WT ClC-0 and the C212S mutant at different pH values. (A) Whole oocyte currents of the WT and C212S at three external pH. See MATERIALS AND METHODS for the voltage protocol to examine the slow-gate inactivation. Dotted lines represent zero-current level. (B) Quasi steady-state inactivation curve of the WT (left, n = 3) and the C212S mutant (right, n = 4) at pH 7.6 (circles), 9.6 (triangles), and 5.6 (squares).

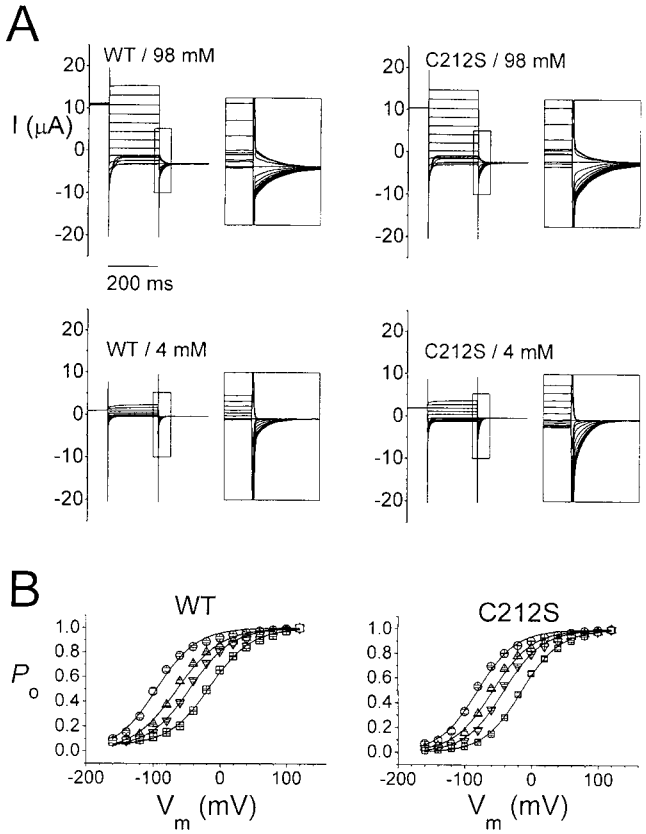

FIGURE 2. Effect of the external Cl^- concentration on the fast gating of the WT channel and the C212S mutant. (A) Whole-cell current of the WT- and C212S-injected oocytes at 98 and 4 mM $[Cl^-]_o$. Voltage protocol is as described in MATERIALS AND METHODS with a maximal depolarized voltage of +120 mV. (Insets) Expanded current traces corresponding to those within the squares to demonstrate the initial current of the fast gating relaxation at −100 mV. (B) Steady-state P_o-V curve of WT and C212S at various $[Cl^-]_o$. Symbols are as follows: ○, 98 mM; Δ, 30 mM; ▽, 15 mM; and □, 4 mM. Solid curves were drawn according to a Boltzmann equation: $P_o = P_{min} + (1 - P_{min})/[1 + \exp(-zF(V - V_{1/2})/RT)]$, with z = 0.8–1.2, P_{min} = 0.03–0.05. $V_{1/2}$'s were as follows: for WT, −91 (98 mM), −60 (30 mM), −42 (15 mM), and −14 mV (4 mM); for C212S, −79 (98 mM), −56 (30 mM), −39 (15 mM), and −12 mV (4 mM).

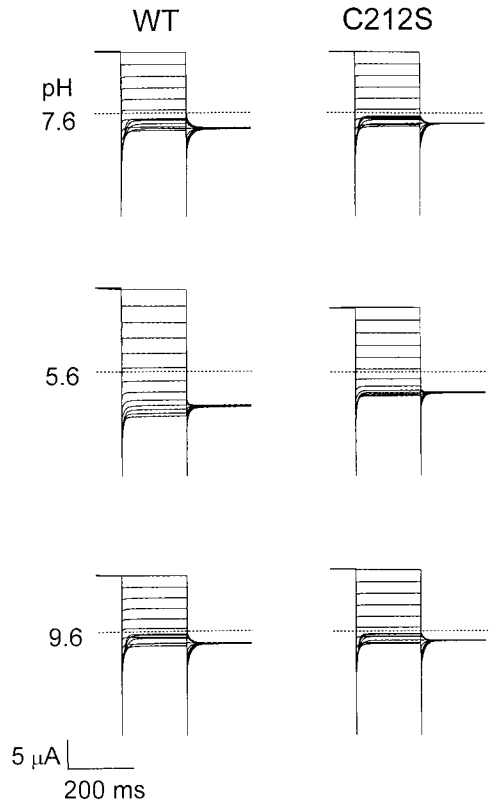

FIGURE 3. External pH effect on the macroscopic current of the WT and the C212S mutant. The recording traces at different pH were from the same oocyte. Voltage protocols are the same as in Fig. 2 A except that a maximal depolarizing test voltage of +80 mV was used. Dotted lines are the zero current level.

anism operates at a time scale of tens to hundreds of seconds at room temperatures (Pusch et al., 1997; Chen, 1998), therefore, it is not difficult to separate the two gating processes under physiological conditions because of a 100- or 1,000-fold difference in their kinetics. However, when the experimental conditions were changed to, for example, low $[Cl^-]_o$ and a nonphysiological pH, ascribing the observed phenomena solely to the effects on the fast gating can become questionable. To ensure that the observed effect was on the fast gating, we simultaneously examined the WT channel and an inactivation-suppressed mutant, C212S. This point mutant has been shown to have a nondetectable inactivation probability. More importantly, its fast-gating properties and the single-channel conductance are not discernibly different from those of the WT channel (Lin et al., 1999). Fig. 1 A shows a comparison of the whole cell current from oocytes expressing the WT channel and the C212S mutant in three external pH conditions. The quasi-steady-state inactivation curves are shown in Fig. 1 B. Although the inactivation of the WT channel is prominent and is subjected to alteration by the external pH (Fig. 1 B, left), the inactivation of C212S, whether in acidic, neutral, or alkaline pH, appears to be suppressed (Fig. 1 B, right).

Fast Gating of C212S Is Identical with that of the WT Channel

To ensure that C212S can be used to study the fast gating of ClC-0, we further compared the responses of the fast gating of WT and C212S to different $[Cl^-]_o$. Fig. 2 A shows macroscopic currents in the presence of 98 and 4 mM $[Cl^-]_o$. For the WT channel, the maximal tail current at 4 mM $[Cl^-]_o$ is smaller than that at 98 mM $[Cl^-]_o$. In C212S, the situation is reversed; the maximal tail current at 4 mM $[Cl^-]_o$ is larger. The inactivation of C212S is also suppressed at low $[Cl^-]_o$ (data not shown). Thus, the bigger inward tail current at 4 mM than at 98 mM $[Cl^-]_o$ results from a larger electrochem-

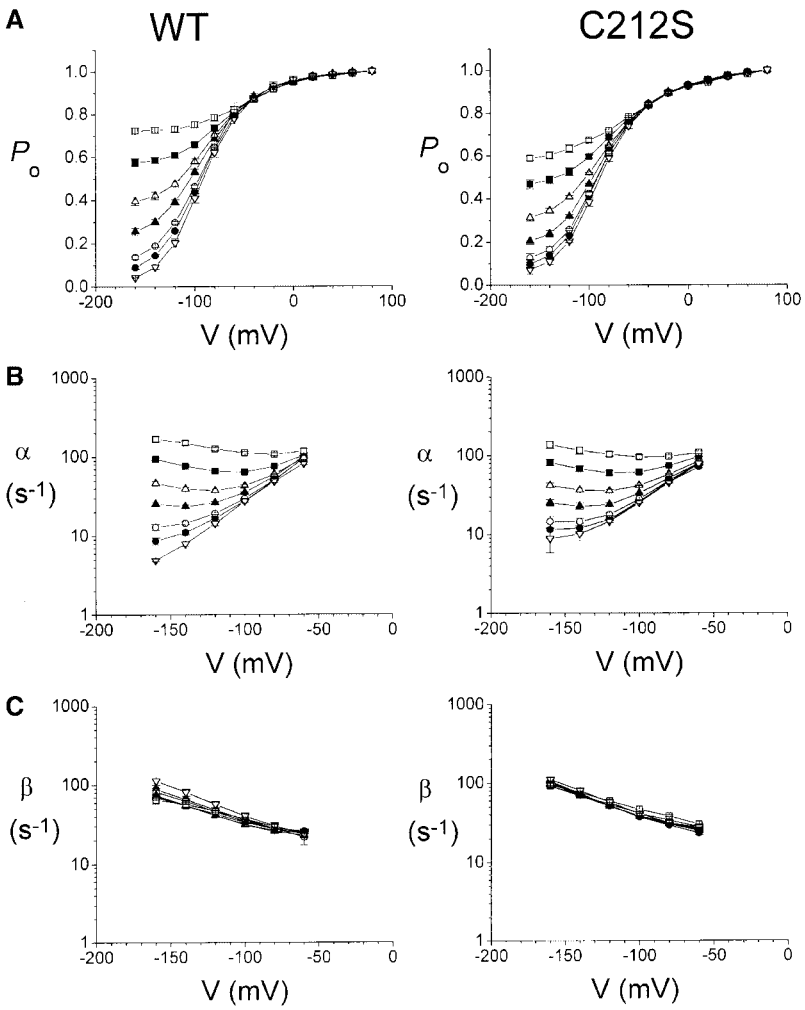

FIGURE 4. Fast-gating properties of the WT and C212S at different external pH values. All parameters were derived from macroscopic current recordings such as those shown in Fig. 3. (A) Effect of pH on the steady-state P_o-V curve. All data were normalized to the initial tail current after a test pulse of +80 mV. (B) Effect of pH on the opening rate of the channels. (C) Effect of pH on the closing rate of the channel. Opening and closing rates were calculated according to Eqs. 1a and 1b. Symbols and the pH were as follows: □, 5.1; ■, 5.6; Δ, 6.1; ▲, 6.6; ○, 7.1; ●, 7.6; and ▽, 9.6. Data points were connected by short straight lines.

ical driving force that pushes Cl^- out of the cell at −100 mV. On the other hand, a smaller tail current at 4 mM $[Cl^-]_o$ in the WT channel reflects a higher inactivation probability at low $[Cl^-]_o$ (Chen and Miller, 1996).

To examine the fast gating of the WT and C212S, we systemically varied $[Cl^-]_o$ and performed a series of experiments similar to those shown in Fig. 2 A. The P_o-V curves at various $[Cl^-]_o$ are plotted in Fig. 2 B, in which the curve shifts to more depolarized voltages when $[Cl^-]_o$ is reduced. For the WT channel, the $V_{1/2}$ of the fitted P_o-V curve changes by ∼20–30 mV with a fourfold reduction in $[Cl^-]_o$. In C212S, the degree of the shift is not significantly different. These results indicate that WT and C212S have similar $[Cl^-]_o$-dependent fast-gating properties. The responsible Cl^- binding sites are likely to be intact in the inactivation-suppressed mutant, C212S.

Effects of External pH on the Fast Gating: Macroscopic Current Recordings

The influences of external pH on the fast gating of WT and C212S are compared in Fig. 3. At neutral pH, the macroscopic current deactivates according to a single-exponential function in response to membrane hyperpolarization. The deactivated currents at various negative voltages usually cross with each other, a hallmark of ClC-0 current. When the pH is increased from 7.6 to 9.6, the time constant and the steady-state component of the current deactivation are not significantly changed. On the other hand, the proportion of the steady-state component increases significantly as the pH is decreased from 7.6 to 5.6. Consequently, the deactivating currents do not cross with each other in this acidic condition. Fig. 4 A shows the P_o-V curves derived from the experiments similar to those shown in Fig. 3. The effect of H^+ is prominent only when the pH is changed from neutral to acidic conditions. Reducing the external pH elevates the open probability of the channel mostly at the hyperpolarized voltages. This behavior is similar to the pH effect on the fast-gate P_o-V curve of ClC-1 (Rychkov et al., 1996). To obtain a mechanistic insight into this H^+ modulation, we derived the opening rate, α, and the closing rate, β, of the fast gate from the current deactivation time constants and the

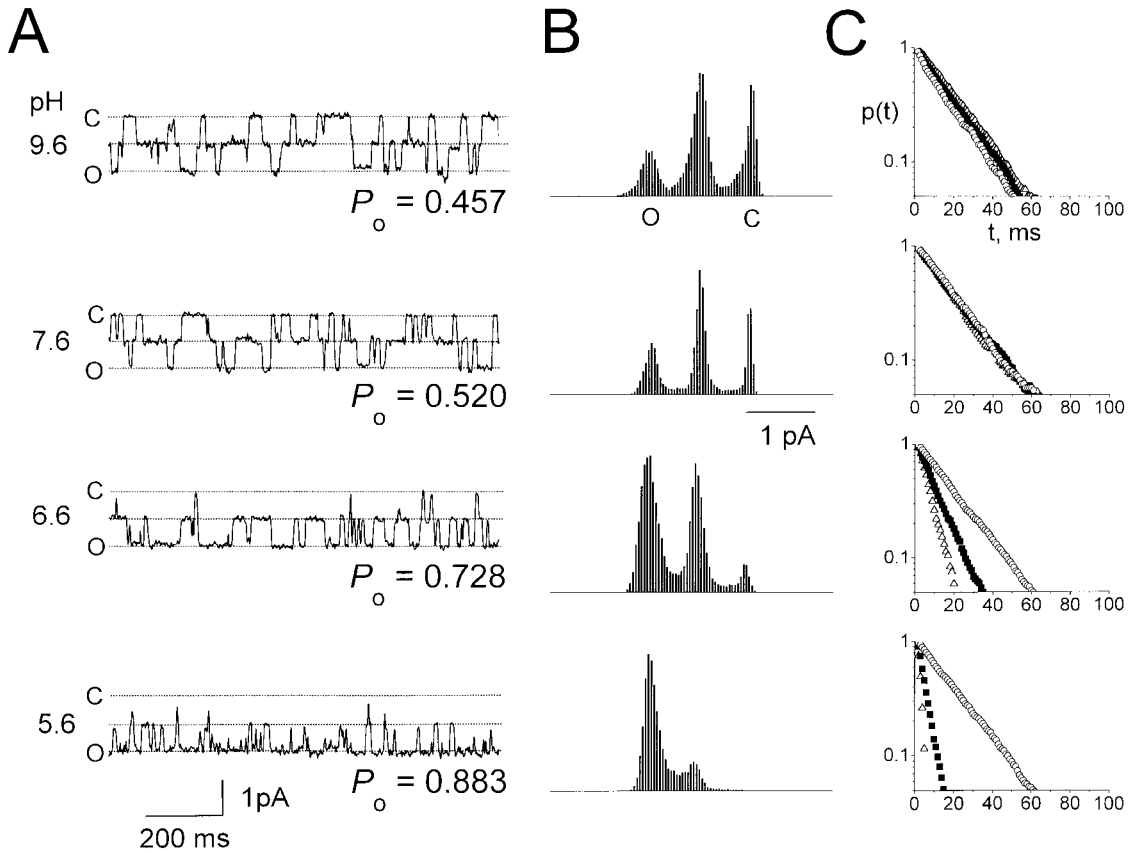

FIGURE 5. Single-channel recordings of C212S at different external pH. (A) Single-channel recording traces at the indicated external pH. Dotted lines are the assigned three current levels. C, closed state of the channel; O, fully open state of the channel. (B) All points amplitude histograms compiled from 30 s (pH 9.6), 30 s (7.6), 40 s (6.6), and 40 s (5.6) recording traces containing the example segments shown in A. The measured state probabilities (f_0, f_1, and f_2) are as follows: (pH 9.6) 0.298, 0.491, and 0.211; (pH 7.6) 0.232, 0.496, and 0.272; (pH 6.6) 0.071, 0.402, and 0.527; (pH 5.6) 0.010, 0.214, and 0.776, resulting in the calculated P_o values shown in A. Assuming a binomial distribution, the predicted state probabilities (f_0, f_1, and f_2) calculated from P_o are as follows: for pH 9.6, 0.295, 0.496, and 0.209; for pH 7.6, 0.230, 0.499, and 0.270; for pH 6.6, 0.074, 0.396, and 0.530; and for pH 5.6, 0.014, 0.206, and 0.780. (C) Dwell-time distributions of the events at the three current levels. Same traces as in B. Δ, ■, and ○ represent the closed (level 0), intermediate (level 1), and fully open (level 2) current levels, respectively. The fitted time constants (τ_0, τ_1, and τ_2) are as follows (in ms): for pH 9.6, 19.5, 18.8, and 17.6; for pH 7.6, 17.5, 19.9, and 18.7; for pH 6.6, 6.6, 10.9, and 19.8; and for pH 5.6, 1.8, 4.3, and 20.3. As discussed in MATERIALS AND METHODS, because there are only 140 closed events at pH 5.6 in this analysis and their durations are heavily affected by the cutoff frequency, the estimate of τ_0 at this acidic condition may have a relatively large error.

steady-state open probabilities (see MATERIALS AND METHODS). Fig. 4 (B and C) indicates that external H^+ profoundly increases the opening rate of the fast gate, whereas the closing rate is almost not affected. The effect of H^+ on the opening rate, again, is more prominent as the membranes become more hyperpolarized.

Effects of External pH on the Fast Gating: Single-channel Recordings

To directly observe the channel behavior in response to external H^+, we performed single-channel recordings on excised inside-out patches. Representative single-channel recording traces of C212S are shown in Fig. 5 A. It is obvious by observing the recording traces or by comparing the all-points amplitude histograms (Fig. 5 B) that the channel conductances at various external pH are all the same. The areas of the all-points amplitude histograms or the measured state probabilities of the three current levels (see Fig. 5 B legend) also reconfirm the conclusion that the P_o of the fast gate is increased mainly as the condition moves from neutral to acidic pH. Dwell-time distributions of the three current levels (Fig. 5 C) reveal that the averaged duration of the fully open events is not significantly affected, whereas the time constants of the distributions of the closed and the intermediate current levels are changed upon altering the external pH. Similar results of the H^+ modulation were also observed on single WT channels (data not shown). The collected open probabilities, opening, and closing rates of C212S are depicted in Fig. 6 (A–C, respectively). To a first degree of ap-

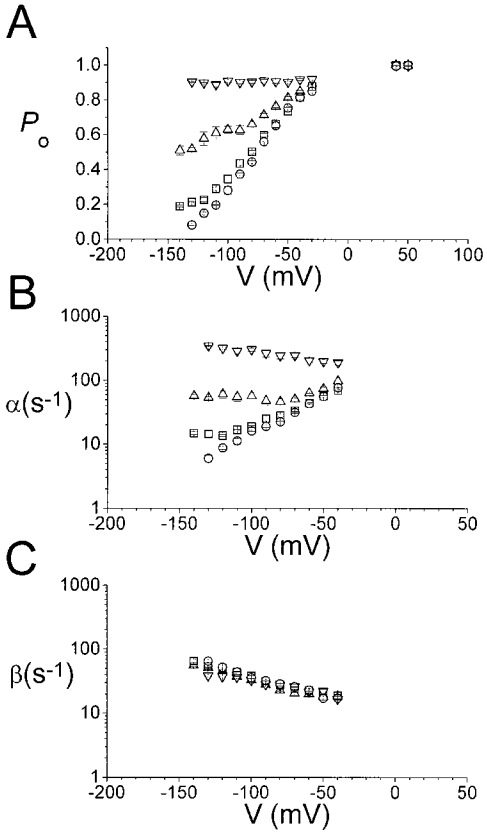

FIGURE 6. Fast gating properties of single C212S channels at different external pH. (A) Steady-state open probability. (B) Opening rate of the fast gate. (C) Closing rate of the fast gate. All rate constants were calculated according to Eqs. 3c and 3d. External pHs were as follows: ▽, 5.6; Δ, 6.6; □, 7.6; and ○, 9.6.

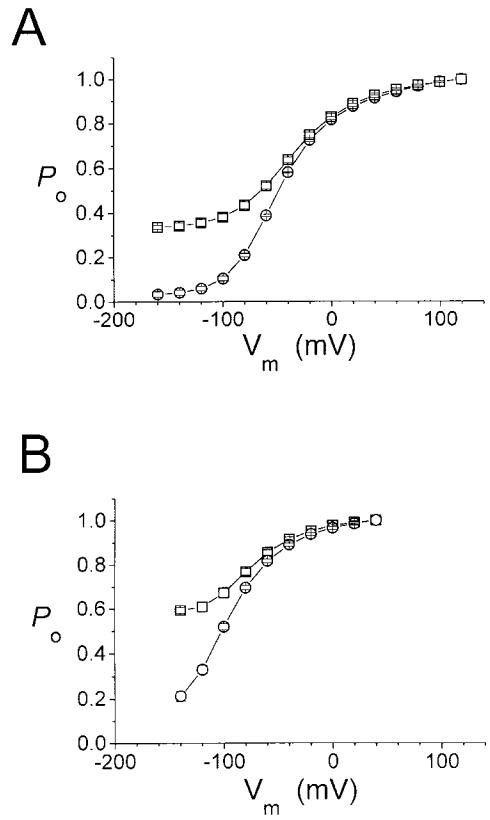

FIGURE 7. External H^+ modulation of the fast gate P_o-V curve of C212S at saturating and nonsaturating $[Cl^-]_o$. Data were derived from macroscopic current recordings at pH 7.6 (○) and 5.6 (□). (A) Comparison of the P_o-V curves under different pH at 15 mM $[Cl^-]_o$ (n = 3). (B) Comparison as performed in A at 300 mM $[Cl^-]_o$ (n = 3–4). Data points were connected with short straight lines.

proximation, the results from the single-channel experiments recapitulate the macroscopic current recordings except a larger minimal P_o. This difference between the macroscopic and single-channel recordings is probably due to a different internal Cl^- concentration in these two recording conditions (Chen and Miller, 1996; Ludewig et al., 1997). However, the key observations with respect to the external H^+ modulation are similar in the macroscopic and single-channel recordings; that is, the closing rate is not affected, whereas the opening rate increases with a lower pH at hyperpolarized voltages. This results in a higher minimal P_o of the P_o-V curve. At depolarized potentials, the opening rates from different pH tend to converge to the same value. This external H^+ effect is fundamentally different from external Cl^- modulation because varying $[Cl^-]_o$ shifts the P_o-V curve in parallel along the voltage axis (Pusch et al., 1995; Chen and Miller, 1996).

H^+ Modulations at Saturating and Nonsaturating $[Cl^-]_o$

The binding site for the $[Cl^-]_o$-dependent fast-gate opening has an apparent Cl^- binding affinity of ~50 mM (Chen and Miller, 1996). With $[Cl^-]_o$ of 150–300 mM, the effect of Cl^- on the fast gating is nearly saturated (Pusch et al., 1995; Chen and Miller, 1996; Lin and Chen, 2000). If external H^+ modulates the fast gating through increasing the Cl^- binding affinity, the effects should not be equal under different $[Cl^-]_o$. Specifically, one would expect a bigger H^+ effect at nonsaturating than at saturating $[Cl^-]_o$. Fig. 7 (A and B) shows such experiments in which the fast-gate P_o-V curves are compared at 15 or 300 mM $[Cl^-]_o$. Comparison of the P_o at −140 mV shows that the modulation effect of H^+ at 300 mM $[Cl^-]_o$ is slightly bigger than that at 15 mM $[Cl^-]_o$. With 300 mM $[Cl^-]_o$, the P_o increases from 0.21 at pH 7.6 to 0.59 at pH 5.6, whereas the P_o at 15 mM $[Cl^-]$ increases from 0.04 to 0.34 with the same pH change. The difference by ~0.2 in P_o between 300 and 15 mM $[Cl^-]_o$ at both pH values is, again, due to an unequal internal Cl^- concentration at these two $[Cl^-]_o$. Nevertheless, the increase in P_o (0.38) in response to a low pH at the saturating $[Cl^-]_o$ is no less than that (0.30) at the nonsaturating $[Cl^-]_o$. Thus, these results do not support the assertion that external H^+ affects the fast gating through modulating the $[Cl^-]_o$-dependent gating mechanism.

DISCUSSION

We have shown that C212S mutant can be used to study the fast gating of ClC-0. The mutation suppresses the inactivation of ClC-0, but the mutant channel retains normal channel conductance and fast-gating properties, including voltage dependence and modulations by external Cl^- (Fig. 2) and pH (Figs. 3 and 4). Therefore, we are confident that the conclusions drawn with respect to H^+ modulation on the fast gating of C212S can be applied to the WT channel.

The effect of external H^+ on the fast gating is mainly on the opening rate, whereas the closing rate is insensitive to the pH change. Higher $[H^+]_o$ increases the opening rate, but the modulation is larger at hyperpolarized voltages. In effect, the P_o-V curve shows a larger minimal P_o when pH is reduced. This phenomenon is different from the effect obtained by varying $[Cl^-]_o$, which shifts the P_o-V curve along the voltage axis (Fig. 2). With such a difference even at the level of a qualitative description of the P_o-V curve, it is already difficult to believe that external H^+ modulates the fast gating through protonation of the Cl^- binding site. To examine this problem more rigorously, we compared the H^+ effect at a nonsaturating (15 mM) and at a nearly saturating $[Cl^-]_o$ (300 mM). Experimental results show that H^+ does not have a smaller modulatory effect in a saturating $[Cl^-]_o$ condition (Fig. 7). This result strongly supports the idea that H^+ modulation of the fast gating is unlikely to be due to an increase in the affinity of the Cl^- binding site responsible for the $[Cl^-]_o$-dependent channel opening.

In a previous single-channel recording study, the fast gate of ClC-0 was found to consist of two opening processes with opposite voltage dependence (Chen and Miller, 1996). In one, the opening is favored by membrane depolarization and is intimately associated with the binding of Cl^- from the external solution. It was hypothesized that when the Cl^- binding site is occupied, the bound Cl^- was further transferred through the membrane electric field to an inner binding site to open the channel. Because Cl^- carries a negative charge, this inward movement of the permeant ion was thought to be the source of the voltage dependence of the opening process (Chen and Miller, 1996). As a result, the channel tends to open more when the membrane is depolarized. The other mechanism contributing to the opening of the fast gate does not involve external Cl^-. The rate of this type of channel opening process, in contrast to the aforementioned $[Cl^-]_o$-dependent mechanism, is faster when the membrane is hyperpolarized. This opening process is obscure, but it is the mechanism that maintains the fast-gate P_o at a nonzero value even at extremely negative voltages (Chen and Miller, 1996; Ludewig et al., 1997).

As the effect of external H^+ modulation is more prominent at more negative voltages, we suspect that H^+ is acting on this $[Cl^-]_o$-independent opening process. To explore this possibility, we adopt a five-state scheme to describe the summation of the above two fast-gate opening processes:

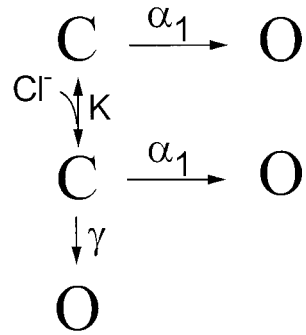

(SCHEME I)

This five-state scheme simplifies the described previously six-state model (Chen and Miller, 1996) by lumping together the inward movement of the bound Cl^- and the subsequent channel opening step. As the Cl^- movement is the rate limiting step, γ determines the opening rate in this $[Cl^-]_o$-dependent process. The rate constant α_1 represents the rate of the hyperpolarization-favored opening process. The observed opening rate α, thus, is the sum of α_1 and γ weighted by a factor determined by $[Cl^-]_o$ and the Cl^- dissociation constant K (Chen and Miller, 1996):

$$\alpha(V) = \alpha_1(V) + \gamma(V)([Cl^-]_o/K)/(1 + [Cl^-]_o/K), \quad (4)$$

where the rate parameters vary with voltage according to Eqs. 5a and 5b:

$$\alpha_1(V) = \alpha_1(0)\exp(z_{\alpha 1}FV/RT), \quad (5a)$$

$$\gamma(V) = \gamma(0)\exp(z_{\gamma}FV/RT). \quad (5b)$$

If H^+ modulation is solely acting on α_1, we should be able to describe the effect of pH on the fast-gate opening rate by varying the value of α_1 but keeping all the other parameters unchanged. In modeling this condition, we applied the values of all parameters shown in Table II of Chen and Miller (1996); i.e., $K = 50$ mM, $\alpha_1(0) = 2.4\ s^{-1}$ (pH = 7.6), $\gamma\ (0) = 446\ s^{-1}$, $z_{\alpha 1} = -0.29$, and $z_{\gamma} = 0.7$. $[Cl^-]_o$ is 98 mM in this study. Fig. 8 A shows that such a model indeed provides a good approximation. When the value of $\alpha_1(0)$ is increased presumably by protonation, the observed opening rates are enhanced mostly at hyperpolarized voltages. At depolarized voltages, in contrast, the opening rates at different external pH converge to the same value.

To gain a structural insight into this H^+ modulation

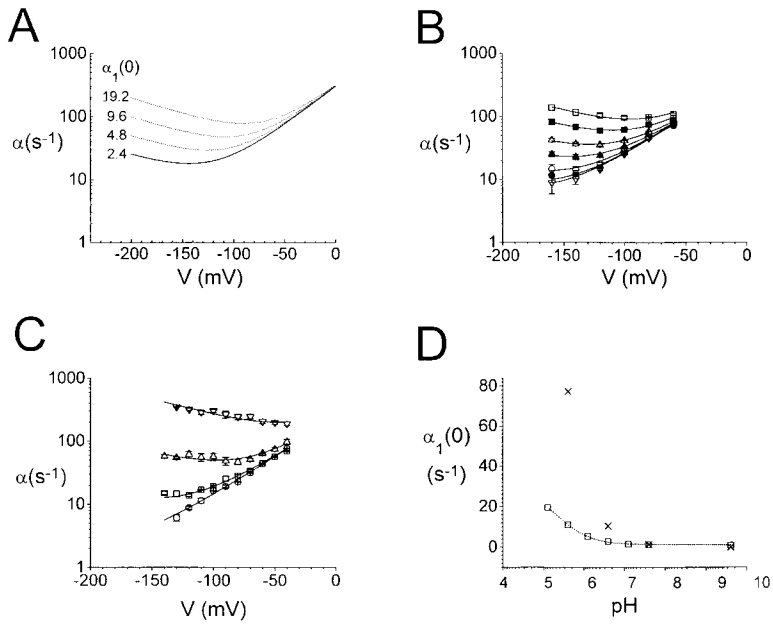

FIGURE 8. External H^+ activates the hyperpolarization-favored opening process. (A) Modeling the fast-gate opening rate according to Scheme I. The solid curve was generated according to Eq. 4, using the values listed in Table II of Chen and Miller (1996). See DISCUSSION for the value of each parameter. Dotted curves were synthesized by increasing the value of $\alpha_1(0)$ as shown on the left of each curve. (B and C) Examination of the fast-gate by the sum of two opening processes. Opening rate data were taken from macroscopic (B) and single-channel recordings (C) as those shown in Figs. 4 B and 6 B, respectively. The dataset at each external pH was fitted to Eq. 4 constrained with a shared value of $\gamma(0)$. Only $\alpha_1(0)$ and $\gamma(0)$ were allowed to vary in the simultaneous multiple-curve fitting process. All the other parameters were the same as those in A. The fitted $\gamma(0)$ were 590 s^{-1} and 340 s^{-1} in B and C, respectively. (D) The fitted $\alpha_1(0)$ from B (□) and C (X) as a function of external pH. Data points from macroscopic recordings were further fitted to a logistic function, $A_1 + (A_2 - A_1)/(1 + [H^+]_o/K_a)$, where K_a is the dissociation constant of the protonation site for H^+. The minimal (A_1) and maximal (A_2) $\alpha_1(0)$ were 0.85 s^{-1} and 31.6 s^{-1}, respectively. The fitted K_a is 4.7×10^{-6} M, corresponding to $pK_a = 5.3$.

site, we fitted the observed opening rates to Eq. 4 (Fig. 8, B and C). Curve fitting for data at different pH was performed at the same time with a shared value of $\gamma(0)$ for each dataset. The fitted values of $\gamma(0)$, either from the macroscopic current recordings or from the single-channel experiments, vary only within a factor of 2 from that reported in Chen and Miller (1996). More importantly, these curve fittings show that the change in the observed opening rate can be well described by varying only one parameter, $\alpha_1(0)$, indicating that the modulation of external H^+ can be explained by an effect on the hyperpolarization-favored opening process. The fitted $\alpha_1(0)$'s in these analyses were plotted in Fig. 8 D as a function of external pH. Curve fitting by a logistic function gives a pK_a of ~5.3 for the protonation site. However, this number can only be viewed as an approximated pK_a value of the titratable site because the titration curve is not saturated even at the most acidic pH in which reliable data can be obtained.

The results presented in this study also raise an interesting possibility that internal Cl^- may interact with external H^+ to modulate the hyperpolarization-activated fast gating. A comparison of the external H^+ modulations between the macroscopic and single-channel experiments shows that the effect is bigger with a higher $[Cl^-]_i$ (compare Fig. 4 with Fig. 6). This can be better seen in Fig. 8 D, in which the fitted $\alpha_1(0)$ in single-channel experiments ($[Cl^-]_i$ = 120 mM) is more than fivefold larger than that obtained from the macroscopic current recordings ($[Cl^-]_i$ ~40 mM) at an external pH of 5.6. An increase of $[Cl^-]_i$ is known to raise the minimal P_o of the fast-gate P_o-V curve (Chen and Miller, 1996; Ludewig et al., 1997; also see Fig. 7). Although this effect was shown to be largely due to a reduction of the closing rate, a slight increase of the opening rate at the hyperpolarized voltage range was also reported at a neutral pH (see Fig. 10 of Chen and Miller, 1996). In the present study, the internal Cl^- effect on the opening rate is also small at a neutral or alkaline external pH as can be seen from a similar $\alpha_1(0)$ between macroscopic and single-channel experiments (Fig. 8 D). However, the difference in the fitted $\alpha_1(0)$ between these two types of experiments becomes larger when the external pH is more acidic. Because $[Cl^-]_i$ in the whole oocyte recordings are not precisely known, these observations remain only qualitative. It will require a better control of $[Cl^-]_i$ to explore the exact functional role of internal Cl^- in the hyperpolarization-favored fast gating and to examine the possible coupling between the actions of H^+ and Cl^-.

In summary, external H^+ modulates the fast gate of ClC-0 in a way similar to that observed in ClC-1. The effect is to enhance the opening rate, leading to an increase in the fast-gate P_o mostly at the hyperpolarized voltages. This modulation of the fast-gate opening, however, is different from that produced by the external Cl^-. External Cl^- increases the depolarization-favored opening rate, whereas H^+ modulates the hyperpolarization-activated fast-gating. These two opening processes, which not only have opposite voltage dependence, but also show characteristic modulations by different external small ions, should be considered together to properly describe the fast-gate openings of the muscle-type ClC channels.

We thank Miss Yu-Wen Lin for participating in some experiments at the early stage of this study.

This work was partly supported by grant NHRI-GT-EX89B813CS from the National Health Research Institutes in Taiwan.

Submitted: 8 January 2001
Revised: 17 May 2001
Accepted: 18 May 2001

REFERENCES

Bauer, C.K., K. Steinmeyer, J.R. Schwarz, and T.J. Jentsch. 1991. Completely functional double-barreled chloride channel expressed from a single *Torpedo* cDNA. *Proc. Natl. Acad. Sci. USA*. 88: 11052–11056.

Chen, T.-Y. 1998. Extracellular zinc ion inhibits ClC-0 chloride channels by facilitating slow gating. *J. Gen. Physiol.* 112:715–726.

Chen, T.-Y., and C. Miller. 1996. Nonequilibrium gating and voltage dependence of the ClC-0 Cl^- channel. *J. Gen. Physiol.* 108:237–250.

Fahlke, C., T. Knittle, C.A. Gurnett, K.P. Campbell, and A.L. George, Jr. 1997. Subunit stoichiometry of human muscle chloride channels. *J. Gen. Physiol.* 109:93–104.

Hanke, W., and C. Miller. 1983. Single chloride channels from *Torpedo* electroplax: activation by protons. *J. Gen. Physiol.* 82:25–45.

Hamill, O.P., A. Marty, E. Neher, B. Sakmann, and F.J. Sigworth. 1981. Improved patch-clamp techniques for high-resolution current recording from cells and cell-free membrane patches. *Pflügers Arch.* 391:85–100.

Hille, B. 1992. Introduction. *In* Ion Channels of Excitable Membranes. 2nd ed. B. Hille, editor. Sinauer Associates, Inc., Sunderland, MA. 1–20.

Hodgkin, A.L., and P. Horowicz. 1959. The influence of potassium and chloride on the membrane potential of single muscle fibers. *J. Physiol.* 148:127–160.

Hodgkin, A.L., and P. Horowicz. 1960. The effect of sudden changes in ionic concentrations on the membrane potential of single muscle fibers. *J. Physiol.* 153:370–385.

Hutter, O.F., and D. Noble. 1960. The chloride conductance of frog skeletal muscle. *J. Physiol.* 151:89–102.

Hutter, O.F., and S.M. Padsha. 1959. Effects of nitrate and other anions on the membrane resistance of frog skeletal muscle. *J. Physiol.* 146:117–132.

Hutter, O.F., and A.E. Warner. 1967. The pH sensitivity of the chloride conductance of frog skeletal muscle. *J. Physiol.* 189:403–425.

Hutter, O.F., and A.E. Warner. 1972. The voltage dependence of the chloride conductance of frog muscle. *J. Physiol.* 227:275–290.

Jentsch, T.J., T. Friedrich, A. Schriever, and H. Yamada. 1999. The CLC chloride channel family. *Pflügers Arch.* 437:783–795.

Jentsch, T.J., W. Günther, M. Pusch, and B. Schwappach. 1995. Properties of voltage-gated chloride channels of the ClC gene family. *J. Physiol.* 482:19S–25S.

Jentsch, T.J., K. Steinmeyer, and G. Schwarz. 1990. Primary structure of *Torpedo marmorata* chloride channel isolated by expression cloning in *Xenopus* oocytes. *Nature.* 348:510–514.

Lin, Y.-W., C.-W. Lin, and T.-Y. Chen. 1999. Elimination of the slow gating of ClC-0 chloride channel by a point mutation. *J. Gen. Physiol.* 114:1–12.

Lin, C.-W., and T.-Y. Chen. 2000. Cysteine modification of a putative pore residue in ClC-0: implication for the pore stoichiometry of ClC chloride channels. *J. Gen. Physiol.* 116:535–546.

Ludewig, U., T.J. Jentsch, and M. Pusch. 1997. Analysis of a protein region involved in permeation and gating of the voltage-gated *Torpedo* chloride channel ClC-0. *J. Physiol.* 498:691–702.

Ludewig, U., M. Pusch, and T.J. Jentsch. 1996. Two physically distinct pores in the dimeric ClC-0 chloride channel. *Nature.* 383: 340–343.

Maduke, M., C. Miller, and J.A. Mindell. 2000. A decade of CLC chloride channels: structure, mechanism, and many unsettled questions. *Annu. Rev. Biophys. Biomol. Struct.* 29:411–438.

Middleton, R.E., D.J. Pheasant, and C. Miller. 1994. Purification, reconstitution, and subunit composition of a voltage-gated chloride channel from *Torpedo* electroplax. *Biochemistry.* 33:13189–13198.

Middleton, R.E., D.J. Pheasant, and C. Miller. 1996. Homodimeric architecture of a ClC-type chloride ion channel. *Nature.* 383:337–340.

Miller, C. 1982. Open-state substructure of single chloride channels from *Torpedo* electroplax. *Phil. Trans. R. Soc. Lond.* B299:401–411.

Miller, C., and E.A. Richard 1990. The *Torpedo* chloride channel: intimations of molecular structure from quirks of single-channel function. *In* Chloride Transporters. A. Leefmans and J. Russel, editors. Plenum Press, New York. 383–405.

Miller, C., and M.M. White. 1980. A voltage-dependent chloride conductance channel from *Torpedo* electroplax membrane. *Ann. NY Acad. Sci.* 341:534–551.

Miller, C., and M.M. White. 1984. Dimeric structure of single chloride channels from *Torpedo* electroplax. *Proc. Natl. Acad. Sci. USA.* 81:2772–2775.

O'Neill, G.P., R. Grygorczyk, M. Adam, and A.W. Ford-Hutchinson. 1991. The nucleotide sequence of a voltage-gated chloride channel from the electric organ of *Torpedo californica. Biochim. Biophys. Acta.* 1129:131–134.

Pusch, M., and T.J. Jentsch. 1994. Molecular physiology of voltage-gated chloride channels. *Physiol. Rev.* 74:813–825.

Pusch, M., U. Ludewig, and T.J. Jentsch. 1997. Temperature dependence of fast and slow gating relaxations of ClC-0 chloride channels. *J. Gen. Physiol.* 109:105–116.

Pusch, M., U. Ludewig, A. Rehfeldt, and T.J. Jentsch. 1995. Gating of the voltage-dependent chloride channel ClC-0 by the permeant anion. *Nature.* 373:527–531.

Rychkov, G.Y., M. Pusch, D. St J. Astill, M.L. Roberts, T.J. Jentsch, and A.H. Bretag. 1996. Concentration and pH dependence of skeletal muscle chloride channel ClC-1. *J. Physiol.* 497:423–435.

Rychkov, G.Y., D. Astill, B. Bennetts, B.P. Hughes, A.H. Bretag, and M.L. Roberts. 1997. pH-dependent interactions of Cd^{2+} and a carboxylate blocker with the rat ClC-1 chloride channel and its R304E mutant in the Sf-9 insect cell line. *J. Physiol.* 501:355–362.

Rychkov, G.Y., M. Pusch, M.L. Roberts, T.J. Jentsch, and A.H. Bretag. 1998. Permeation and block of the skeletal muscle chloride channel, ClC-1, by foreign anions. *J. Gen. Physiol.* 111:653–665.

Saviane, C., F. Conti, and M. Pusch. 1999. The muscle chloride channel ClC-1 has a double-barreled appearance that is differentially affected in dominant and recessive myotonia. *J. Gen. Physiol.* 113:457–467.

Steinmeyer, K., C. Ortland, and T.J. Jentsch. 1991. Primary structure and functional expression of a developmentally regulated skeletal muscle chloride channel. *Nature.* 354:301–304.